ELSEVIER

International Journal of Solids and Structures 41 (2004) 2349–2362

INTERNATIONAL JOURNAL OF SOLIDS and STRUCTURES

www.elsevier.com/locate/ijsolstr

Shock-induced structural transitions and dynamic strength of solids

Yu.I. Mescheryakov *, A.K. Divakov, N.I. Zhigacheva

Institute of Problems of Mechanical Engineering, Russian Academy of Sciences, V.O. Bol'shoi ave., 61, Saint-Petersburg 199178, Russia

Received 27 October 2003; received in revised form 27 October 2003

Abstract

Shock tests of series of materials under uniaxial strain conditions including constructional and armor steels, aluminum alloy, copper and beryllium, show that spall-strength sensitively depends on the structural instability of material under compression at the front of compressive pulse. This instability is shown to be a shock-induced structural transition which results in irreversible mesostructure formation in solid. It is also shown that value of structural instability threshold under dynamic compression measured in uniaxial strain tests determines a strength-component of resistance of material to high-velocity penetration in Alekseevskii–Tate model.

Keywords: Structural instability; Mesoscopic scale; Spallation; Penetration

1. Introduction

Spall fracture of material is known to be a result of interference of release waves propagating from rear surfaces of impactor and target. Under certain ratio between thickness of impactor and target a tensile stress generates inside the target, which results in spallation (Glushak et al., 1992). A common thread is that spall-strength is a sufficiently objective characteristic of tensile strength of material at the microsecond region of dynamic loading. In reality, however, a preliminary compression of material takes place during passing the front of compressive pulse. If dynamic compression achieves a critical value, the irreversible structural changes of solid occur before the tensile stresses generate within spall zone of target. Thus, dynamic failure during spallation sensitively depends on plastic instability of a material under compression at the front of loading pulse. The plastic instability can be considered as a strain-rate dependent structural phase transition by means of which the shock self-consistently establishes the scale features at the mesoscopic scale. A possibility for existence of similar structures has been theoretically studied by Aero (2000). Micro-deformation model based on solution to non-linear sine-Helmholtz equation predicts a non-stable

* Corresponding author. Tel.: +7-812-321-4765; fax: +7-812-321-4771.
E-mail address: ymesch@impact.ipme.ru (Yu.I. Mescheryakov).

0020-7683/$ - see front matter © 2003 Elsevier Ltd. All rights reserved.
doi:10.1016/j.ijsolstr.2003.11.015

Nomenclature

ρ	density of material (g/cm^3)
U_{imp}	velocity of impactor (m/s)
W	pull-back velocity (m/s)
U_{A}	free surface velocity corresponding to instability threshold (m/s)
D	mean velocity fluctuation (square root of the particle velocity dispersion) (m/s)
u_{fs}	current free surface velocity (m/s)
v	current particle velocity
C_{l}	longitudinal sound velocity (m/s)
σ_{HEL}	elastic precursor stress (GPa)
H_{D}	dynamic hardness (GPa)
Y_{D}	dynamic yield limit (GPa)
v	Poisson coefficient
R	strength-component of resistance of target to high-velocity penetration (GPa)
Y	strength-component of resistance of penetrator (GPa)

behavior of crystalline lattice subjected to shear deformation in non-linear elastic region of loading. This instability leads to nucleation of large-scale structures such as mesorotations, shear bands and their combinations. The large-scale structures nucleate long before a transition to macroscopical plasticity happens. If the strain gradient does not exceed some critical value, the large-scale structures may disappear, i.e. the described structural transition appears to be reversible at that stage. At higher strain gradients a bifurcation transition takes place, which results in nucleation of structures of mesoscopical scale commonly seen in microstructural investigations.

Initiation of the plastic instability under compression is determined by the competition between rates of accumulation and relaxation of internal stresses at the mesoscopic scale. The specifics of structure rearrangements of dynamically deformed material reveals via the shock-induced change of the particle velocity distribution (dispersion), which is thought to be a quantitative characteristics of the energy exchange between mesoscopic and macroscopic scale levels measured in real time in non-equilibrium processes (Asay and Barker, 1974; Mescheryakov and Divakov, 1994). Specifically, when the mesoparticle velocity dispersion at the shock front grows faster than mean mass velocity, the internal energy goes on the formation of new formations at other structural scale. In the presented paper, on example of shock loading of series of materials, the effect of processes at the front of compressive pulse on dynamic strength of materials during spallation and penetration is explored.

2. Kinetic characteristics of mesostructure

Because the experimental investigations presented here are based on a statistical approach to multiscale processes in dynamically deformed solids, we present a definition of variables that characterize the stochastic medium behavior at the mesolevel. The description of such a kind medium is grounded on the concept of physical kinetics for the particle velocity distribution function, or probability density commonly used in the mechanics of fluid and gas. According to definition of the particle velocity distribution function, the quantity $f(\mathbf{r}, \mathbf{v}, t)\,\mathrm{d}\mathbf{v}\,\mathrm{d}\mathbf{r}$ represents the mathematical expectation of the number of particles in the volume $\mathrm{d}\mathbf{r}$ at the position $\mathbf{r}$ that have velocities in the range from $\mathbf{v}$ to $\mathbf{v} + \mathrm{d}\mathbf{v}$ at the time t. The normalization

condition requires that integrating over the physical and particle-velocity spaces gives the total number of particles

$$\int_{-\infty}^{\infty} f(\mathbf{r},\mathbf{v},t)\,\mathrm{d}\mathbf{r}\,\mathrm{d}\mathbf{v} = \boldsymbol{N}(t). \tag{1}$$

It follows from the normalization condition that the value $n(\mathbf{r},t)$, which is determined by the relation

$$n(\mathbf{r},t) = \int f(\mathbf{r},\mathbf{v},t)\,\mathrm{d}\mathbf{v} \tag{2}$$

is the number density of mesoparticles. For the mass density one obtains

$$\rho(\mathbf{r},t) = m\int f(\mathbf{r},\mathbf{v},t)\,\mathrm{d}\mathbf{v}, \tag{3}$$

where m is the mass of the particle.

Hydrodynamic flow of a medium is characterized by the velocity of mass transport. We define the mean mass velocity at the position $\mathbf{r}$ and time t by relation

$$\mathbf{u}(\mathbf{r},t) = \frac{1}{\rho(r,t)}mn(\mathbf{r},t)\langle\mathbf{v}\rangle, \tag{4}$$

where

$$\langle\mathbf{v}(\mathbf{r},t)\rangle = \frac{1}{n(r,t)}\int \mathbf{v}\boldsymbol{f}\ (\mathbf{r},\mathbf{v},t)\,\mathrm{d}\mathbf{v} \tag{5}$$

In order to characterize the fluctuative properties of dynamically deformed heterogeneous medium, one can use the velocity dispersion

$$\boldsymbol{D}^2 = \int (\mathbf{v}-\mathbf{u})^2 f(\mathbf{r},\mathbf{v},t)\,\mathrm{d}\mathbf{v}. \tag{6}$$

For our purposes, it seems to be convenient in analysis of experimental results, together with dispersion, to use the square root of the mesoparticle velocity dispersion, D, which here and henceforth calls *mean velocity fluctuation*. This is the important quantitative characteristic of mesostructure kinetics, which, together with the free surface velocity profile $\mathbf{u}(t)$, characterizes the response of solid on impact in planar experiments.

The first statistical moment of the particle velocity distribution function, i.e. the average particle velocity $\mathbf{u}(\mathbf{r},t)$, characterizes the macroscopic behavior of medium under dynamic strain conditions. Commonly used free-surface velocity profiles measured by means of gauges or a "VISAR" (a particular laser-interferometer configuration for measuring particle velocity) contain only information about the average behavior of material. Mesoscopic effects such as shear banding and mesorotations are determined by higher order statistical moments, such as particle velocity dispersion and excess, i.e. asymmetry of the velocity distribution function. Their values provide a statistical characterization of the relative velocities of mesoparticles. This means that, when speaking about mesoparticle dispersion under conditions of dynamic deformation, one cannot determine the specific form (dislocation groups, shear bands, tilt boundaries, rotations etc.) of elementary carriers of deformation at the mesolevel.

Nevertheless, it is not too hard to estimate their typical scale by using the principles of interference used to measure the particle velocity dispersion. Measurement of the particle velocity dispersion is based on the concept that different particles at the free surface of the target, and lying within the laser beam spot, give different Doppler frequency shifts. Effective interaction of individual particles and laser radiation is possible only when the dimension of the particle significantly exceeds the laser radiation wavelength (approximately

10 times). On the other hand, uniform broadening of the radiation spectrum is achieved only if there is a sufficient number of similar particles within the diameter, $d_{b,}$ of the laser beam spot on the free surface of target. From this, the diameter, d_p, of the particle is estimated to fall in the range

$$\lambda \ll d_p \ll d_b. \tag{7}$$

As a rule, the laser beam has a transverse dimension about of 70–100 μm at its focal point on the free surface of a target, whereas the laser radiation wave length is approximately 0.6 μm. In this case, the size of the particle lies in the range from 7 to 10 μm. In accordance with a generally accepted classification (Panin et al., 1982), this size belongs to mesoscopic scale level.

The mesoparticle velocity distribution resulting in broadening the reflected laser radiation spectrum leads, in turn, to a decrease of the interference fringe contrast, which gives quantitative information about the particle velocity dispersion at the mesolevel (Asay and Barker, 1974; Mescheryakov and Divakov, 1994). When the mesolevel is subdivided into two sublevel, elementary carriers of deformation for the sublevels may suffer their own particle velocity distributions. In this case there may be three different situations depending on the degree of the velocity distribution at these levels

(a) Particle velocity dispersion at the mesolevel-1 is greater than that at the mesolevel-2.
(b) Particle velocity dispersion at the mesolevel-2 is greater than that at the mesolevel-1.
(c) The dispersion values at these two levels are identical.

These cases are presented in Fig. 1 in the form of velocity-space configurations. The laser beam of the interferometer being focused on the free surface of the target just corresponds to the meso-2 scale level. In

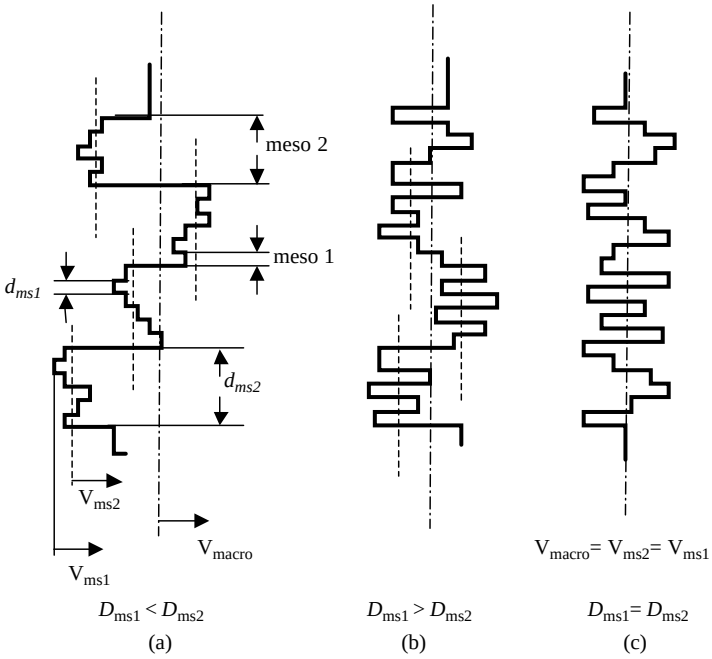

Fig. 1. Velocity-space configuration of shock-wave front for different mutual values of velocity dispersion at the mesolevel-1 and mesolevel-2.

Table 1
Results of uniaxial shock tests of 40XCHMA steel

No. shot	h_t (mm)	h_i (mm)	U_{imp} (m/s)	U_{fs}^{max} (m/s)	D (m/s)	W (m/s)	U_A (m/s)
1	5.35	1.98	211	196.1	4	166.1	196.2
2	5.30	2.00	215	202.8	2	168.7	198.5
3	5.36	1.96	290	261	7.6	199.1	256
4	5.06	2.00	307	291.3	8.5	192.3	287.4
5	5.59	1.95	309	279.8	9.3	195.8	276
6	5.25	1.98	329	297	10	195.1	291.6
7	5.26	2.15	356	336.5	11.7	197.6	324.4
8	5.20	1.99	379	345	16.1	200.9	335.8
9	5.35	1.99	405	383.3	21.5	214.1	365.9
10	4.83	1.97	437	408.9	19.5	200.3	388.7

other word, when the laser interference technique is used, one deals with the velocity history for an individual element of mesolevel-2. This means that the macroscopic particle velocity, u_{av}, which results from averaging the particle velocity distribution at the mesolevel-2 coincides with the average particle velocity at the mesolevel-1 only when the particle velocity dispersions for the meso-1 and meso-2 scale levels are equal. In all the other cases, the macroscopic velocity can be obtained from averaging the velocity distribution at the mesolevel-2. For that purposes, simultaneous monitoring of the free surface of the target at several points, as developed by Barker (2000) or on some square of the free surface (Trott et al., 2001) can be used.

3. Experimental technique and results

The experiments on shock loading of different solids under uniaxial strain conditions within impact velocity range of 50–600 m/s were performed by using a one stage light gas gun facility of 37 mm bore diameter. In the majority of experiments the thickness of target and impactor were adjusted to provide spallation. The free surface velocity profiles were recorded with two-channel velocity interferometer (Mescheryakov and Divakov, 1994). Besides the free surface velocity profiles, $u_{fs}(t)$, the experimental technique provides a recording of time history of distribution (dispersion) in particle velocity during shock deformation, $D^2(t)$. According to this approach, the shock-wave front is considered as averaged motion of deformed medium at the background of which the velocity fluctuations take place at one or more scale levels (see Fig. 1). Results of shock test for 40XCHMA are provided in Table 1. Thicknesses of target and impactor are in the second and third columns of table, respectively. The fourth column is the impactor velocity in symmetrical collision, when impactor is produced from the same material as target. Maximum free surface velocity at the plateau of compressive pulse is given in the fifth column. Mesoparticle velocity distribution width at the mesoscopic scale level-1 (square root of the velocity dispersion), D, is presented in the sixth column and pull-back velocity W is given in column number seven. At last, the eighth column indicates the free surface velocity which corresponds to change of the first front inclination before it transits into plateau, U_A. The latter value requires a special explanation. In Fig. 2 a free surface velocity profile for 40XCHMA [1] steel is presented. This profile consists of several pieces, which are clearly identified in all the experiments. Piece OA' is the elastic precursor, AA'—plastic front, AB—transient zone, BC—is the smooth piece of loading plastic front, CD—is the plateau of compressive pulse where the particle velocity is invariable, DE—elastic unloading front and EF—plastic unloading front.

[1] We use Russian marking for the materials under investigation.

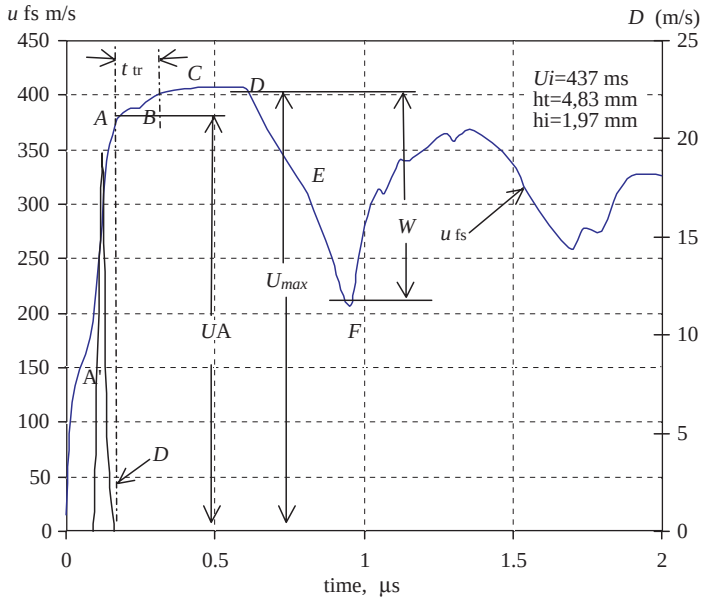

Fig. 2. Free surface velocity profile u_{fs} and velocity dispersion D for 40XCHMA steel target loaded at the impact velocity of 437 m/s.

In this work, the shock tests of series of materials including 38XH3MΦA and 40XCHMA steels, D-16 aluminum alloy, M-2 copper and beryllium were performed. At every and each test, the free surface velocity, $u_{\mathrm{fs}}(t)$, and velocity dispersion profiles, $D(t)$, were registered, and then the dependencies of $U_{\mathrm{A}} = f(U_{\mathrm{imp}})$ and $W = f(U_{\mathrm{imp}})$ on the impact velocity were plotted. The post shocked study of specimens was undertaken to reveal the structure mechanisms of spall fracture.

4. Instability threshold under dynamic compression and spall-strength of solids

Shape of the front of compressive pulse and length of separate pieces of this front are known to reflect a dynamics of processes flowing at the microscopic scale level during the shock-wave passage. The quantitative characteristic of macroscopic response of medium on shock loading is a time-resolved profile of shock wave $u_{\mathrm{fs}}(t)$. Just that profile is commonly registered in the shock tests under uniaxial strain conditions. Quantitative characteristic of fluctuative processes at the microlevel is the temperature as a measure of chaotic motions of atoms. At higher scale levels, such as mesoscopic scale level, the quantitative characteristic of fluctuative features of medium is a velocity dispersion of mesoparticles. The behavior of velocity dispersion during the shock deformation is shown to be sensitively depended on whether or not the shock wave is steady or non-steady (Khantuleva and Mescheryakov, 1999; Mescheryakov, 2002). In the steady waves, the dispersion achieves its maximum value in a middle of plastic front and approaches to zero near the pulse plateau. Presented in Fig. 2 free surface velocity profile shows that inclination of plastic front changes when the velocity dispersion becomes equaled to zero. Beginning from this moment of time, the stress relaxation is realized owing to other, more large-scale mechanism. Initiation of this mechanism happens at point A and continues for a transient stage AB, after that the particle velocity grows again, although much slowly. As a matter of fact, transition to new regime of dynamic deformation can be considered as a structural phase transformation initiated by shock loading. Value of mean particle velocity corresponding to the onset of transient stage, U_{A}, determines a dynamic threshold of structural transition,

which is important strength-characteristic of material under shock compression. Note, that for the ceramics the strength under tension is absent at all, so the strength under compression is the main strength-characteristic.

In Fig. 3 a dependence of the free surface velocity corresponding to the instability threshold on the impactor velocity, $U_A = f(U_{imp})$, for polycrystalline beryllium is presented. One can see that break of dependence occurs at the impact velocity of 120 m/s, after that a slope of the dependence decreases. In this figure a dependence of pull-back velocity, $W = f(U_{imp})$, is also plotted. Spallation begins just at the impact velocity corresponding to break (cusp) of the dependence $U_A = f(U_{imp})$. This means that at the strain rate corresponding to impactor velocity of 120 m/s, irreversible structural changes occurred in the material, which results in change of character of its resistance to shock loading. Structural transitions under dynamic compression are identified for all the studied materials enumerated above. So, in Fig. 4 the analogous dependence for D-16 aluminum alloy is presented. The break of dependence $U_A = f(U_{imp})$ here also coincides with the onset of spallation.

For the plastic materials, such as copper and ductile steel, the break at the $U_A = f(U_{imp})$ dependence corresponds to change of slope of dependence for pull-back velocity, $W = f(U_{imp})$. This is clearly seen in Figs. 5 and 6 where couples of dependencies $U_A = f(U_{imp})$ and $W = f(U_{imp})$ are provided for these materials—the breaks at both dependencies happens simultaneously.

There exists a direct coupling of instability threshold and spall-strength—the higher instability threshold, the higher spall-strength of the material. To check this assertion, two sets of 38ХН3МФА constructional steel targets have been tested under identical shock conditions. The first set of steel targets was as supplied while the second set was subjected to standard for this steel thermal treatment. Results of the tests are presented in Figs. 7 and 8. For the first set of the steel, the structural instability occurs at the impact velocity of 200 m/s while for the second set—at the velocity of 260 m/s. Accordingly, the pull-back velocity after break point changes from 160 to 180 m/s for the first set of steel and from 175 to 200 m/s for the second set. Thus, the spall-strength of material proves to be dependent on the threshold of dynamic instability under compression. Above results also testify that spall-tests do not provide an objective information about tensile strength of solid at the microsecond range of dynamic loading.

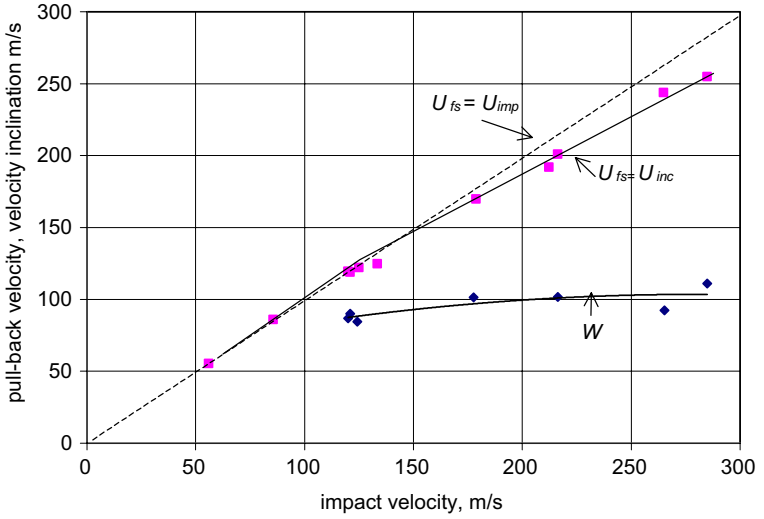

Fig. 3. Instability threshold U_A and pull-back velocity W for beryllium.

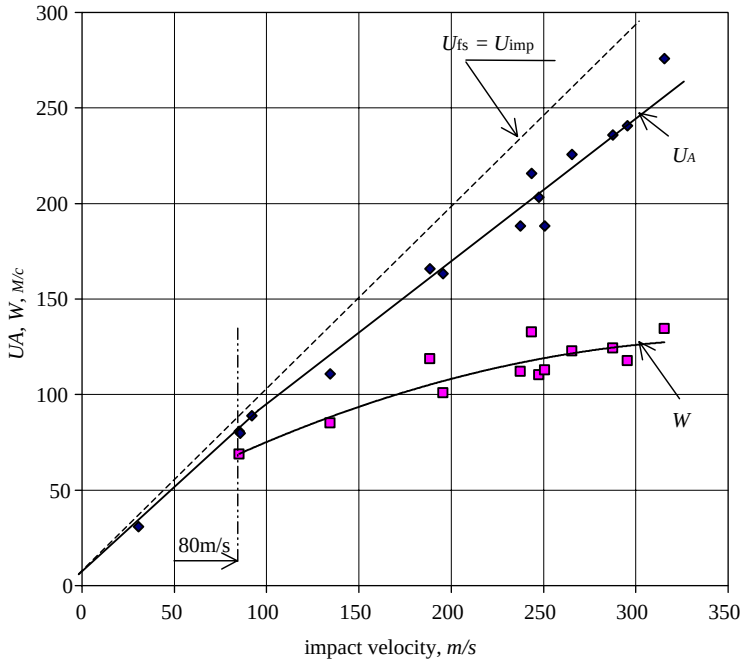

Fig. 4. Instability threshold U_A and pull-back velocity W for D-16 Al alloy.

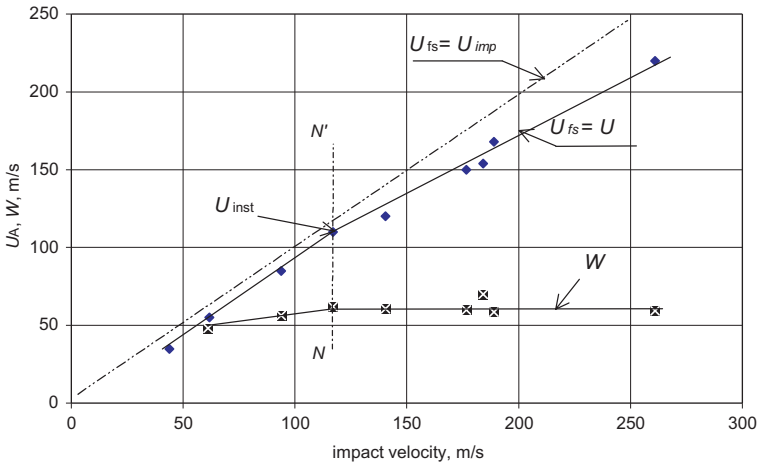

Fig. 5. Instability threshold U_A and pull-back velocity W for M-2 copper.

In the case of steady plastic waves, instability under shock compression is initiated at the impact velocity when the particle velocity dispersion at the mesoscale-1, as a means for relaxation of internal stresses, is entirely exhausted. At that moment, relaxation of internal stresses at higher structural scale, at the so-called mesoscale-2 level, is initiated. Initiation of mesoscopic structural level-2 can flow both in reversible and irreversible manner. To explain the latter assertion, in Fig. 9 the temporal free surface velocity profiles for ductile (armco-iron) and brittle (beryllium) materials registered with velocity interferometer are presented.

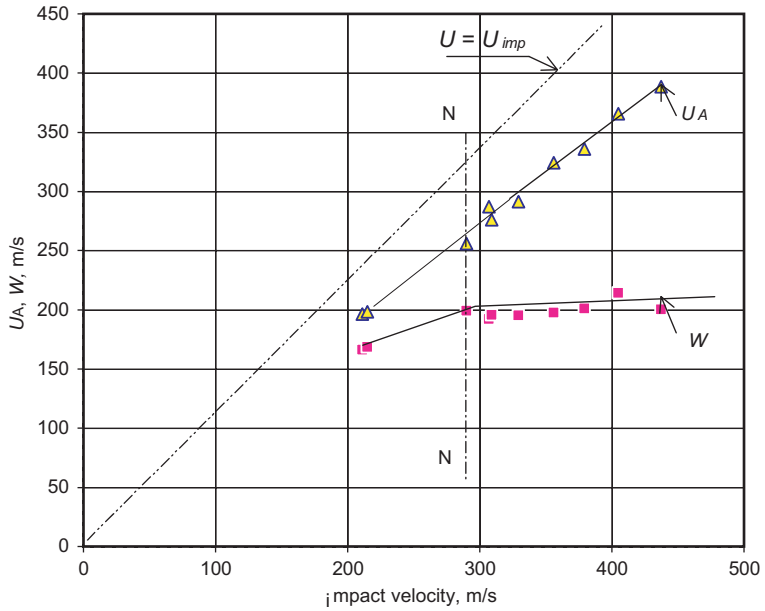

Fig. 6. Instability threshold U_A and pull-back velocity W for 40XCHMA steel.

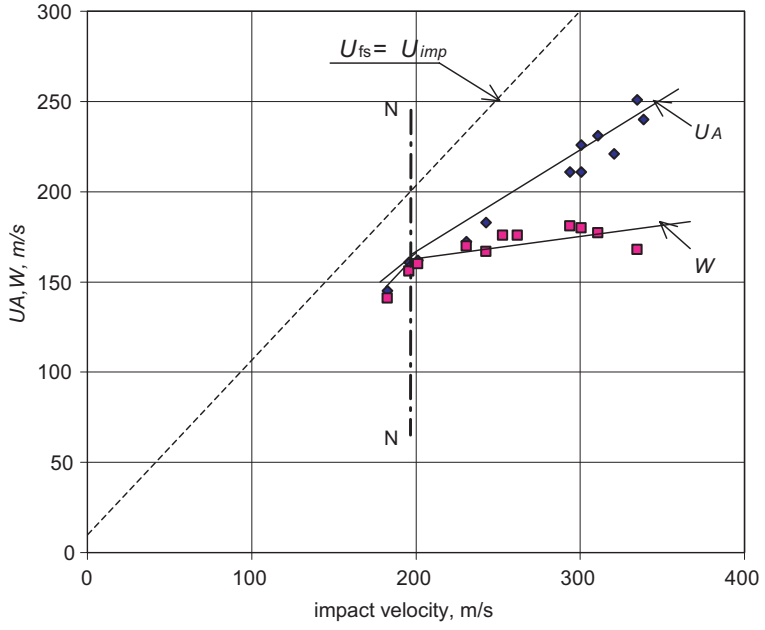

Fig. 7. Instability threshold U_A and pull-back velocity W for 38XH3MΦA steel (1 set).

One can see that the first profile has an evident oscillation structure while the second profile is smooth. Since the cross dimension of laser beam of interferometer approximately coincides with the dimension of structural element of mesoscale-2 (100 μm), oscillations at the mesoscale-2 level just correspond to motions

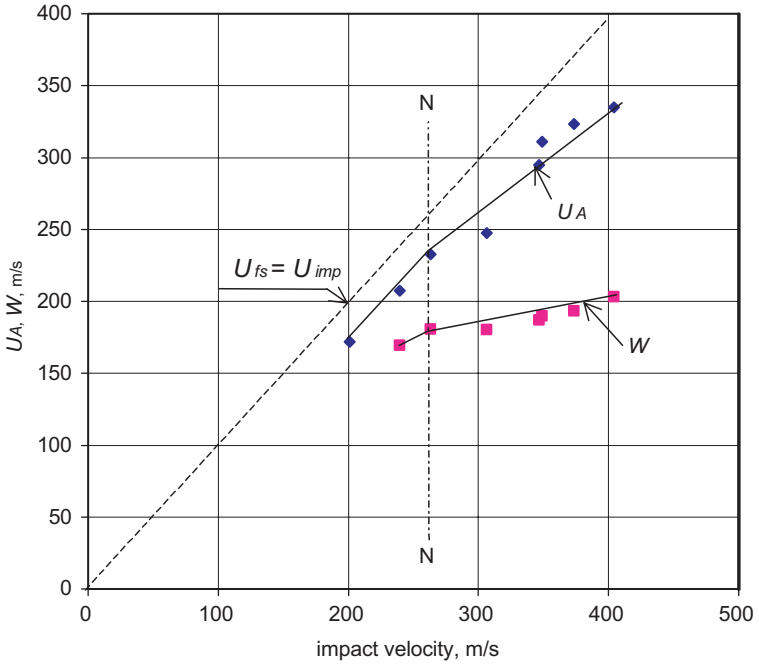

Fig. 8. Instability threshold U_A and pull-back velocity W for 38XH3MΦA steel (2 set).

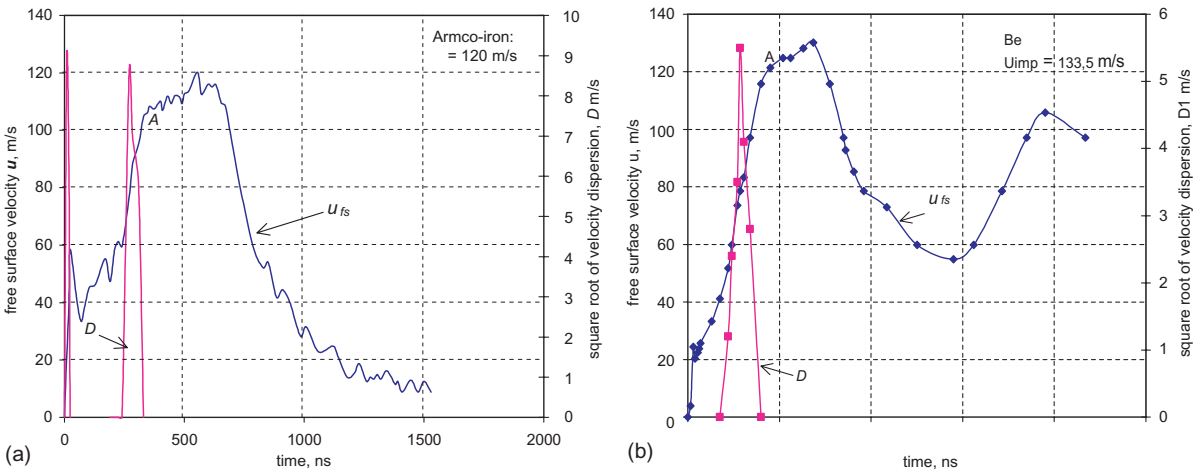

Fig. 9. Free surface velocity profiles $u_{fs}(t)$ and velocity dispersion $D(t)$ for: (a) armco-iron and (b) beryllium.

of one structure element of meso-2 level as a whole, and reflects a relaxation of internal stresses at that scale level. The profile in Armco-iron corresponds to Fig. 1a while the profile in beryllium–to Fig. 1b. In brittle materials the mesoscopic scale-2 below instability threshold is frozen, so relaxation of internal stresses is carried out only due to mobility of structural elements of mesoscale-1. When relaxation ability at the mesolevel-1 is exhausted, a growth of internal stresses takes place up to value sufficient for initiating the mesoscopic scale–2.

5. Structure investigations

The purpose of microstructure investigations is to find a change of mechanism and/or scale of dynamic fracture below and higher instability threshold. In this work we present the results of microstructure investigation for 40XCHMA steel. To perform the microstructural investigations, all the specimens after shock tests were cut on one of planes along the wave propagation direction and after polishing and etching were subjected to studying with optical and SEM-microscopy.

Standard regime of thermal treatment supposes a low tempering so that the structure of the steel consists of martensite plus low bainite. This kind of steel reveals evident features of spallation within overall range of impact velocities. Typical pattern of spallation at the lower boundary of impact velocities is presented in Fig. 10a. Cleavage seems to be most proper mechanism of spallation for lower range of impact velocities. There is plane cracks parallel to free surface of target the length of which ranges from 1.5 to 10 mm. As a rule, the spall crack looks as a continuous horizontal crack having small vertical steps the height of which does not exceed 20 μm.

Similar character of spall fracture takes place up to impact velocity of 290 m/s. New feature appearing at the impact velocity of 307 m/s is a nucleation of regions surrounded by closed crack. Their size ranges from 25 to 200 μm. Typical patterns of such a kind of closed formations are presented in Fig. 10b. At the impact

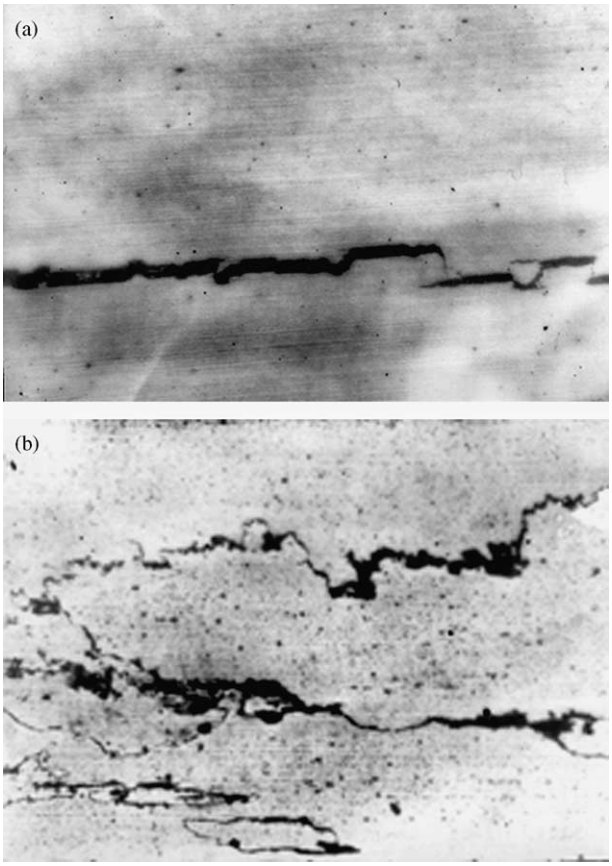

Fig. 10. Spallation in 40XCHMA steel target: (a) cleavage at the impact velocity of 211 m/s (magnification 32^{+}) and (b) nucleation of closed regions and fragmentation within spall zone at the impact velocity of 307 m/s (magnification 32^{+}).

velocity of 356 m/s the internal area of closed regions begins to fragment. Thus, one can fix a following evolution of the fracture process at the spall zone with the increase of impact velocity

(i) Cleavage mechanism—at the impact velocities lower than instability threshold ($U_{\text{imp}} < 307$ m/s).
(ii) Nucleation of closed regions and brittle fragmentation—at the impact velocities higher than instability threshold ($U_{\text{imp}} > 307$ m/s).

6. Instability under dynamic compression and resistance of solids to high-velocity penetration

Normal stress at which irreversible structural transition at the front of compression pulse occurs must be considered as independent strength-characteristic of material determining the threshold instability of material under dynamic compression. This strength-characteristic is thought to be important not only in developing the theoretical models of dynamic fracture but in calculating the parameters of high-velocity penetration processes. The penetration depth is known to be determined on the basis of modified Bernoulli equation (Hohler and Stilp, 1990):

$$Y + \frac{1}{2}\rho_{\text{imp}}(v-u)^2 = \frac{1}{2}\rho_t u^2 + R. \tag{8}$$

Here v is the impactor velocity, u is the particle velocity in the material of target, Y and R are the empirical constants defining a dynamic strength for the material of penetrator and target, respectively. In the well-known reviews on high-velocity penetration it is claimed that physical meaning of parameters Y and R remains to be unclear (Hohler and Stilp, 1990). Value R takes into account a deviation in behavior of the material of target from the hydrodynamic model of penetration. Micromechanisms of dynamic deformation responsible for physical nature and value of R are the subject of investigations on microplasticity. The parameter R is often identified with dynamic hardness H_{D} which connected to dynamic yielding limit, Y_{D}, by the following correlation dependence (Tate, 1967; Lasarev et al., 1993):

$$H_{\text{D}} = (3 - 3.5)Y_{\text{D}}. \tag{9}$$

In turn, dynamic yielding limit is determined by Hugoniot elastic limit, σ_{HEL}

$$Y_{\text{D}} = \frac{1-2v}{1-v}\sigma_{\text{HEL}}, \tag{10}$$

where v is the Poisson coefficient.

The main conclusion following from the analysis of peculiarities of high-velocity penetration, and also from the analysis of experimental data, is that the strength-component of resistance of solids to penetration, as a complementary factor for the inertial forces, is determined by the resistance to plastic deformation. This means that if the character of plastic deformation changes, for example, because of change of structural mechanism of deformation, the strength-component of resistance to penetration changes as well.

The high-velocity penetration tests do not provide quantitative information about change of macroscopic response of target on impact due to change of the mechanism of plastic deformation. Analysis of shock-wave processes during penetration shows that inside the target, in vicinity of the head of penetrator, at the so-called stagnation point (critical point of flows within target near the penetrator), the uniaxial strain conditions are realized (Hohler and Stilp, 1990). At the moment of impact, a shock wave of nearly one-dimensional strain at three-dimensional stress is produced at the interface between the rod projectile and target. As distinct from the high-velocity penetration, shock-wave tests under uniaxial strain conditions are sufficiently informative. This permits to apply the results obtained under planar collision experiments as a strength-characteristic of target for penetration tests. In this case, as strength-components of resistance of

Table 2
Comparison of strength-component of resistance to high-velocity penetration R and instability threshold for different materials

Material of target	U_{HEL} (m/s)	R (Tate) (GPa)	C_{pl} (mm/s)	U_A (m/s)	σ_i (uniaxial strain) (GPa)
D-16 Al alloy	40	0.6	5.35	80	0.58
M-2 copper	5	2.44	4.38	132	2.54
383XH3MΦA steel	75	4.01	5.0	210	3.96

target to penetration R, the stress corresponding to the instability threshold of material under compression may be taken

$$R = \sigma_i = \tfrac{1}{2}\rho_t C_{pl} U_A. \tag{11}$$

C_{pl} is the velocity of plastic front in uniaxial strain tests and U_A is the particle velocity corresponding to loss of structure stability under compression at the front of pulse.

In Table 2 the results of calculation of value R by using formulae (9) and (10), on one hand side, and formula (11), on other hand side, are presented for the set of constructional materials which have been tested under uniaxial strain conditions. The stress value at the elastic precursor was also obtained in the planar shock tests. It is seen from the table that R values determined according Tate's technique, and dynamic instability threshold values determined under planar tests are practically coincide for all the material tested. This means that strength-component of material resistance to high-velocity penetration has a concrete physical meaning—its value is determined by the structural instability threshold of material under uniaxial strain conditions.

7. Summary

Analysis of the processes at the front of compression pulse and microstructure investigations show that spall-tests do not provide an objective information on the tension strength of material in microsecond region of dynamic loading. The spall-strength proves to be sensitively depends on whether or not the irreversible processes of structural stability loss at the front of pulse occur.

The threshold of structural instability of material under shock compression determines a strength-component of resistance of material to high-velocity penetration of rods into target.

Acknowledgements

The work was performed in the frame of Grant FPC of Ministry of Industry and Science of Russian Federation no. 40.010.11.1195 and VW Research Project 1/74 645.

References

Aero, E.L., 2000. Microscale deformation in two-dimensional lattice: structural transitions and bifurcations at critical shear. Phys. Solid State 42, 1147–1153 (Trans. from Fizika Tverdogo Tela, 2000, 42, 1113–1119).

Asay, J.R., Barker, L.M., 1974. Interferometric measurement of shock-induced internal particle velocity and spatial variations of particle velocity. J. Appl. Phys. 45, 2540–2546.

Barker, L.M., 2000. Multi-beam VISAR for simultaneous v/s time measurements. In: Furnish, M.D., Chhabildas, L.C., Nixon, R.S. (Eds.), Shock Compression of Condensed Matter. APS, Melville, New York, pp. 999–1002.

Glushak, B.P., Kuropatenko, V.F., Novikov, S.A., 1992. Investigation of material strength under dynamic loading. Nauka (Russian), Novosibirsk.

Hohler, V., Stilp, A.J., 1990. Long-rod penetration mechanics. In: Zukas, J.A. (Ed.), High Velocity Impact Dynamics. John Wiley and Sons, New York (ISBNO-471-51444-G).

Khantuleva, T.A., Mescheryakov, Yu.I., 1999. Nonlocal theory of the high-strain-rate processes in structured media. Int. J. Solids Struct. 36, 3105–3129.

Lasarev, V.B., Balankin, A.S., Isotov, A.D., Kozhushko, A.A., 1993. Structural Stability and Dynamic Strength of Inorganic Materials. Nauka (Russian), Moscow.

Mescheryakov, Yu.I., Divakov, A.K., 1994. Multiscale kinetics of microstructure and strain-rate dependence of materials. Dymat. J. 1 (4), 271–287.

Mescheryakov, Yu.I., 2002. Meso-macro-energy exchange in shock deformed and fractured solids. In: Horie, Y.Y, Davison, L., Thadhani, N.N. (Eds.), High Pressure Shock Compression of Solids VI. Old Paradigms and New Challenges. Springer-Verlag, Berlin, pp. 169–213.

Panin, V.E., Grinyaev, V.Yu., Elsukova, T.F., Ivanchin, A.G., 1982. Structural levels of deformed solids. Isvest. Vuz. Fiz. 6, 5–22.

Tate, A., 1967. A theory for the deceleration of long rods after impact. J. Mech. Phys. Solids 15, 387.

Trott, W.M., Chhabildas, L.C., Baer, M.R., Castaneda, J.N., O'Hare, J.J., 2001. Investigation of dispersive waves in low density sugar and HMX using line-imaging velocity interferometry. Bull. Am. Phys. Soc. 46, 31.